2.18 (m (br), 2 H, $CpCH_2CH_2NHCOCH_3$), 1.52 (s (br), 3 H, $CpCH_2CH_2NHCOCH_3$). Crystals of neither derivative were suitable for X-ray diffraction studies.

Attempted Photoproduction of H_2. A solution of $[(CpCH_2CH_2NH_3^+)_2Mo_2(CO)_6][NO_3^-]_2$ (1.4 mM), PTA (10 mM), and 1,1'-dicarboxycobaltocenium hexafluorophosphate (12 mM) in 100 mL of pH 2 buffer was prepared in a 100-mL Schlenk flask. The headspace on the flask was approximately 1 mL. The solution was irradiated for 30 min with magnetic stirring. A 50-μL aliquot of the cover gas was analyzed by GC every 5 min. Only a small amount of CO was detected, and no H_2 was detected. Similar results were obtained in analogous experiments in pH 7 and pH 2 solutions with and without PTA or the 1,1'-dicarboxycobaltocenium.

Detection of CO_2. A CO_2- and O_2-free pH 12 aqueous NaOH solution (10 mL) of the $(CpCOOH)_2W_2(CO)_6$ dimer (20 mM) and $Na_3[P(C_6H_5SO_3^-)_3]$ (200 mM) was prepared in a septum-capped test tube. The tube was irradiated for 30 min while the solution was magnetically stirred. A cannula was used to connect the test tube (A) to another test tube (B) containing 4 mL of a clear saturated aqueous solution of $Ba(OH)_2$. The solution containing the photolysis products was acidified with 2 mL of 6 M H_2SO_4. Effervescent was immediate, and bubbles could be seen going through the $Ba(OH)_2$; the solution in B gradually became cloudy. The precipitate in test tube B was vacuum filtered, dried in an oven, and analyzed by IR spectroscopy (KBr pellet). The product was identified as $BaCO_3$ by comparison with an authentic sample. In a quantitative experiment, 7.9×10^{-5} mol of dimer produced 1.4 mg (7.1×10^{-6} mol) of $BaCO_3$ (10%). H_2 was also formed in 10% yield.[1] A control experiment without $(CpCOOH)_2W_2(CO)_6$ did not produce a precipitate.

Acknowledgment is made to the National Science Foundation for the support of this work. Prof. D. J. Darensbourg is acknowledged for a sample of PTA, and Dr. I. Horvath is acknowledged for helpful discussions. Partial support from the Department of Education Areas of National Need Program for A.A. is acknowledged.

OM920305P

Intramolecular Redox Chemistry of Molecules with Alkyne and CCo_3 Cluster Functionalities: Electronic Interaction and Structural Isomerism in Reduced Clusters with Multiple Redox Centers

Gillian H. Worth, Brian H. Robinson,* and Jim Simpson*

Chemistry Department, University of Otago, P.O. Box 56, Dunedin, New Zealand

Received April 22, 1992

The redox chemistry of the tricobaltcarbon clusters $[CCo_3(CO)_9]_2$, $OC[CCo_3(CO)_9]_2$, and $C_n[CCo_3(CO)_9]_2$ (n = 2, 4), linked by formal single and/or triple carbon–carbon bonds, is contrasted with that of molecules with only a single cluster redox center, $RC_nCCo_3(CO)_9$. The latter clusters undergo a reversible reduction process, whereas molecules with linked clusters display electrochemical responses indicative of interacting redox centers. After the formation of a radical anion, in which the electron is delocalized via the Co_3C–C_n–CCo_3 link, a CE mechanism gives a new species with a reversible redox couple. Spectroscopic evidence suggests that this new species is a bridged-carbonyl isomer of the initial radical anion. Formation of the isomers is attributed to electron delocalization through the carbyne link and steric influence of the equatorial CO groups. An improved synthesis of $[CCo_3(CO)_9]_2$ and the X-ray structure analysis of the compound $(MeO)_3P(CO)_8Co_3CC{\equiv}CCCo_3(CO)_7[P(OMe)_3]_2$, (*Pbca*; a = 18.074 (4) Å, b = 37.534 (7) Å, c = 12.918 (4) Å, Z = 8) are also reported.

Electronic interaction between adjacent organometallic moieties which are readily oxidized or reduced can lead to a range of electron-transfer responses.[1] These responses are normally classified according to the degree to which the interaction brings about a change in physical properties.[2] Redox studies on many transition-metal carbonyl clusters have shown[1,3] that they are structurally flexible electron reservoirs with "tunable" redox properties dependent on the coordination sphere of the metal framework. Extension of this work to systems where the clusters are linked to other redox centers, such as ferrocene, demonstrated that the clusters can participate in electronic interactions which lead to classical mixed-valence molecules.[4] However, interpolation of an electronically saturated system such as CH_2 or SiR_2 between the ferrocene and cluster removes the possibility of electronic communication between the two redox centers.[5] This raised the question of whether intracluster communication could be established if two cluster reactions were directly linked by an unsaturated carbon–carbon bridge, a communication which is well-established in ferrocene chemistry.[6] Controlled thermal decomposition of this type of molecule

(1) Geiger, W. E.; Connelly, N. G. *Adv. Organomet. Chem.* **1985**, *24*, 87.
(2) Robin, M. B.; Day, P. *Adv. Inorg. Chem. Radiochem.* **1980**, *58*, 451. Hush, N. S. *Chem. Phys.* **1975**, *10*, 361.
(3) Robinson, B. H.; Simpson, J. In *Paramagnetic Organometallic Species in Activation/Selectivity, Catalysis*; Chanon, M., Juillard, M., Poite, J. C., Eds.; NATO ASI Series 257; Kluwer: Dordrecht, The Netherlands, 1989; p 357. Lemoine, P. *Ibid.*, p 397.
(4) Colbran, S. B.; Robinson, B. H.; Simpson, J. *J. Chem. Soc., Chem. Commun.* **1982**, 1362.
(5) Borgdorff, J.; Ditzel, E. J.; Duffy, N. W.; Robinson, B. H.; Simpson, J. *J. Organomet. Chem.*, in press.
(6) Cowan, D. D.; Le Vanda, C.; Park, J.; Kaufman, F. *Acc. Chem. Res.* **1973**, *6*, 1. Powers, M. J.; Meyer, T. J. *J. Am. Chem. Soc.* **1978**, *100*, 4393.

0276-7333/92/2311-3863$03.00/0

could also be a route to materials with useful physical properties, a thesis recently illustrated using the molecules described in this paper.[7]

The carbon-capped tricobalt clusters CCo_3 and CCo_3C display several attractive features as redox centers. Both have upper occupied molecular orbitals which have contributions from the metal, capping carbon atoms, and ligands conferring tunable electron reservoir character.[8,9] Thus, with a cyclopentadienyl ligand sphere the CCo_3C moiety is readily oxidized;[10] an all-CO configuration for CCo_3 gives a reducible center,[11] but successive replacement of CO by electron donors ultimately results in an oxidizable center.[12] Molecules with CCo_3C or CCo_3 linked by conducting bridges could therefore provide a variety of redox responses. Furthermore, the carbon cap provides a reaction site for the development of cluster multiplicity.[13,14] A preliminary study of the CCo_3C system has been described;[10] this paper presents an investigation of molecules with interacting CCo_3 centers.

The initial strategy was to utilize acetylene groups to link cluster units via an unsaturated backbone, $(CO)_9Co_3CC_nCCo_3(CO)_9$, but the lability of polyacetylene derivatives limited the usefulness of direct coupling. This prompted an electrochemical investigation of the recently[15] synthesized clusters $RC_2CCo_3(CO)_9$ (I), acetylene-linked

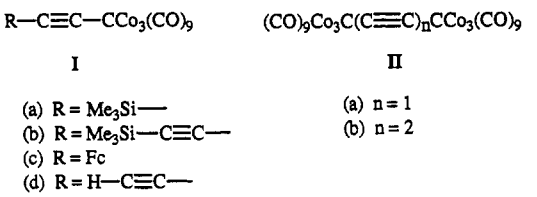

I

(a) R = Me_3Si—
(b) R = Me_3Si—C≡C—
(c) R = Fc
(d) R = H—C≡C—
(e) R = Ph

II

(a) n = 1
(b) n = 2

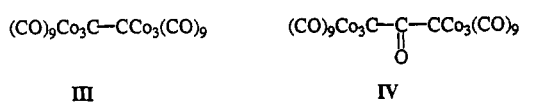

III

IV

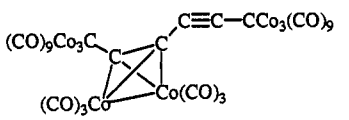

V

clusters (II), and several molecules with linked CCo_3 units (IIa,[16] III,[17,19] IV,[18] V[20]) synthesized by serendipitous routes a number of years ago. Crystallographic studies[20-25] had revealed short C–C bond lengths in the intracluster backbone of the last four molecules, indicative of electron delocalization along the backbone, but the ramifications for the redox properties had not been explored. The influence of the acetylene group and the effect of another adjacent Co_3C unit on the redox properties of tricobalt clusters is described herein.

Experimental Section

All preparations, manipulations, and electrochemical work were carried out under an atmosphere of argon. III–V were prepared by the procedure below or by the thermolysis of $BrCCo_3(CO)_9$.[17,18] Clusters I and II were prepared by coupling reactions between the appropiate alkyne and $BrCCo_3(CO)_9$;[15] ligands and reducing agents were commercial reagents.

ESR spectra were obtained on a Varian E3 spectrometer using in situ electrochemical generation of radical anions, with an efficient three-electrode cell.[26] Electrochemical procedures were as described earlier.[10,27] The reference electrode was a solid Ag/AgCl electrode immersed directly in the solution and was calibrated in situ with the known electrochemically reversible couple [ferrocene]$^{+/0}$, taken as $E_{1/2}$ = 0.68 V in CH_2Cl_2.[26] Scan rates were 20 mV s^{-1} for polarographic and 50 mV s^{-1} to 5 V s^{-1} for voltammetric measurements. Solutions were $\sim 10^{-3}$ M in electroactive material and 0.10 M in supporting electrolyte (tetrabutylammonium hexafluorophosphate) for transient electrochemistry. Bulk electrolyses were carried out using a home-built potentiometer with solutions 10^{-2} M in cluster and supporting electrolyte, the whole apparatus enclosed in an argon-filled plastic bag; samples for spectroscopic analysis were withdrawn by syringe during the experiment. A three-arm cell which could be operated in vacuo or under an argon atmosphere allowed chemical reduction sequences to be monitored by in situ spectroscopic techniques (IR, ESR).

Preparation of $[CCo_3(CO)_9]_2$ (III) and $OC[CCo_3(CO)_9]_2$ (IV). $BrCCo_3(CO)_9$ (2 g), Ph_3As (3.4 g), and hexane (40 cm^3) were sealed in vacuo in a thick-walled tube (volume 115 cm^3), and the tube was heated to 70 °C for 3 h. Orange-brown crystals precipitated on cooling which were collected and washed with cold hexane. The crude product was dissolved in CH_2Cl_2 and the solution placed on a plate coated in silica gel (1:1 CH_2Cl_2/hexane). The major band was removed and crystallized to give a 38% yield of pure III (based on $BrCCo_3(CO)_9$).[19]

The addition of halide scavengers (e.g. Zn dust) or triarylphosphines or diarylstibines did not increase the yield. When the reaction was repeated with the tube containing a partial atmosphere of CO, a 63% yield of $OC[CCo_3(CO)_9]_2$ was obtained with the same workup procedures.

Reactions with Lewis Bases. Monosubstituted derivatives of Ia,c with $P(OMe)_3$ and PPh_3 as ligands were prepared by standard method,[7] in most cases being characterized from spectroscopic data. These data were identical with those for previously described derivatives of $CCo_3(CO)_9$.[28] Products from the reactions of IIa with $P(OMe)_3$ are described in detail below, but related compounds were made with $P(OPh_3)$.[29]

(7) Worth, G. H.; Robinson, B. H.; Simpson, J. *Appl. Organomet. Chem.* **1990**, *4*, 481.
(8) Schilling, B. E. R.; Hoffmann, R. J. *J. Am. Chem. Soc.* **1979**, *101*, 3456. Chesky, P. T.; Hall, M. B. *Inorg. Chem.* **1981**, *20*, 4419. Xiang, S. E.; Bakke, A. A.; Chen, H. W.; Eyermann, C. J.; Hoskins, J. L.; Lee, T. H.; Seyferth, D.; Withers, H. P.; Jolly, W. L. *Organometallics* **1982**, *1*, 689.
(9) Pinhas, A. R.; Albright, T. A.; Hofmann, P.; Hoffmann, R. J. *Helv. Chim. Acta* **1980**, *63*, 929.
(10) Elder, S. M.; Robinson, B. H.; Simpson, J. *J. Organomet. Chem.* **1990**, *398*, 165. Colbran, S. B.; Robinson, B. H.; Simpson, J. *Organometallics* **1984**, *3* 1344.
(11) Bond, A. M.; Peake, B. M.; Robinson, B. H.; Simpson, J.; Watson, D. J. *Inorg. Chem.* **1977**, *16*, 410.
(12) Downard, A. J.; Robinson, B. H.; Simpson, J. *Organometallics* **1986**, *5*, 1122, 1132. Bond, A. M.; Dawson, P. A.; Peake, B. M.; Robinson, B. H.; Simpson, J. *Inorg. Chem.* **1979**, *18*, 1413.
(13) Penfold, B. R.; Robinson, B. H. *Acc. Chem. Res.* **1973**, *6*, 73. Seyferth, D. *Adv. Organomet. Chem.* **1976**, *14*, 97.
(14) Vollhardt, K. P. C. *Angew. Chem., Int. Ed. Engl.* **1980**, *19*, 560.
(15) Worth, G. H.; Robinson, B. H.; Simpson, J. *Organometallics* **1992**, *11*, 501.
(16) Robinson, B. H.; Spencer, J. L. *Chem. Commun.* **1968**, 1480; *J. Chem. Soc. A* **1971**, 2045.
(17) Bor, G.; Marko, L.; Marko, B. *Chem. Ber.* **1961**, *95*, 333.
(18) Allegra, G.; Peronaci, E. M.; Ercoli, R. *Chem. Commun.* **1966**, 549.
(19) Robinson, B. H.; Tham, W. S. *J. Organomet. Chem.* **1968**, *16*, P45.
(20) Dellaca, R. J.; Penfold, B. R.; Robinson, B. H.; Robinson, W. T.; Spencer, J. L. *Inorg. Chem.* **1970**, *9*, 2197.
(21) Robinson, B. H.; Spencer, J. L. *J. Organomet. Chem.* **1971**, *30*, 267.
(22) Dellaca, R. J.; Penfold, B. R.; Robinson, B. H.; Robinson, W. T.; Spencer, J. L. *Inorg. Chem.* **1970**, *9*, 2204.
(23) Brice, M. D.; Penfold, B. R. *Inorg. Chem.* **1972**, *11*, 138.
(24) Allegra, G.; Valle, S. *Acta Crystallogr.* **1969**, *B25*, 107.
(25) Dellaca, R. J.; Penfold, B. R. *Inorg. Chem.* **1971**, *10*, 1269.
(26) Lindsay, P. N. T.; Peake, B. M.; Robinson, B. H.; Simpson, J.; Honrath, U.; Vahrenkamp, H. *Organometallics* **1984**, *3*, 413.
(27) Downard, A. J.; Robinson, B. H.; Simpson, J. *Organometallics* **1986**, *5*, 1140.
(28) Dawson, P. A.; Robinson, B. H.; Simpson, J. *J. Chem. Soc., Dalton Trans.* **1979**, 1762. Matheson, T. W.; Robinson, B. H.; Tham, W. S. *J. Chem. Soc. A* **1971**, 1457.

Table I. Crystal Data, Data Collection, and Refinement of Compound VIb

empirical formula	$C_{28}H_{27}O_{24}P_3Co_6$
mol wt	1194.03
cryst syst	orthorhombic
space group[a]	*Pbca* (No. 61)[a]
a, Å	18.074 (4)
b, Å	37.534 (7)
c, Å	12.918 (4)
V, Å^3	8764 (3)
D_c (D_m), g cm^{-3}	1.81 (1.79)
Z	8
Cryst size, mm	0.44 × 0.40 × 0.32
μ(Mo Kα), cm^{-1}	25.00
F(000)	4752
diffractometer	Nicolet R3M
temp/K	173(5)
radiation	Mo Kα(λ = 0.710 69 Å)
scan type	θ–2θ
scan speed, deg min^{-1}	7.32
data limits, deg	$1 < 2\theta < 50$
rflns measd	*hkl*
cryst decay,[b] %	<6
abs cor[c]	empirical
transmissn	0.831 (max), 0.649 (min)
total no. of rflns	8215
no. of unique data ($I > 2\sigma(I)$)	4168
method of solution	direct
no. of variables	262/316[d]
treatment of protons	calcd
R ($\sum\Delta F/\sum\|F_o\|$)	0.085
R_w ($\sum w^{1/2}(\Delta F)/\sum w^{1/2}F_o$)	0.083
weight (w)	$2.1439/(\sigma^2F + 0.000771F^2)$
residual density, e Å^{-3}	+3.67, −0.99

[a] Reference 30. [b] Standard reflections (660), (6,−6,0), (0,0,12) measured after every 100 reflections. [c] Lorentz and polarization corrections and empirical absorption corrections were applied using the SHELXTL system. [d] Refined in alternating blocked-matrix cycles.

(a) $C_2[CCo_3(CO)_9]_2$. $C_2[CCo_3(CO)_9]_2$ (IIa; 0.034 g) and excess $(MeO)_3P$ (0.111 g) were stirred together in hexane (15 cm^3) at room temperature for 15 h, and the reaction was monitored by TLC. The solvent was removed in vacuo; the product mixture was dissolved in a minimum of CH_2Cl_2, the solution was applied to silica plates, and the plates were developed with hexane/CH_2Cl_2 (1:1). Three major products were eluted. Band 1 recrystallized from hexane gave black rhombs of $C_4Co_6(Co)_{16}[(MeO)_3P]_2$ (VIa). Anal. Calcd for $C_{26}H_{18}Co_6P_2O_{22}$: C, 28.44; H, 1.65. Found: C, 28.74; H, 1.71. ν(CO) (hexane): 2089 (m), 2073 (vs), 2047 (vs), 2029 (m), 2019 (ms), 2007 (vw), 1996 (vw), 1984 (w) cm^{-1}. Band 2, recrystallized from hexane, gave black $C_4Co_6(CO)_{15}[(MeO)_3P]_3$ (VIb). Anal. Calcd for $C_{28}H_{27}Co_6P_3O_{24}$: C, 28.17; H, 2.28. Found: C, 28.22; H, 2.25. ν(CO) (hexane): 2097 (vw), 2079 (ms), 2058 (vs), 2042 (vs), 2029 (vs), 2018 (ms), 2007 (s), 1970 (sh) cm^{-1}. Black crystals obtained from band 3 recrystallized from hexane and were identified as $C_4Co_6(CO)_{14}[(MeO)_3P]_4$ (VIc). Anal. Calcd for $C_{30}H_{36}Co_6P_4O_{26}$: C, 27.92; H, 2.81. Found: C, 28.22; H, 2.95. ν(CO) (hexane): 2064 (m), 2051 (vs), 2034 (w), 2017 (vs), 2008 (w), 2004 (w), 1913 (mw) cm^{-1}.

(b) $[CCo_3(CO)_9]_2$. $[CCo_3(CO)_9]_2$ (III) and $(MeO)_3P$ were stirred together in hexane at various temperatures and different reaction times. In all cases large amounts of dark material precipitated which left pale brown solutions. In no instance did the spectroscopic analysis indicate other than trace quantitites of ligand-substituted cluster, and attempts to isolate solid derivatives were unsuccessful. Similarly, reactions with other phosphites and phosphines did not provide substituted derivatives.

X-ray Structure Determination of VIb. Samples of VIb were prepared as detailed above and were recrystallized from hexane as irregular blocks. Precession photography (Cu Kα radiation) revealed an orthorhombic unit cell, and the systematic absences uniquely defined the space group *Pbca*.[30] The crystals were weakly diffracting, with few reflections observed beyond $2\theta > 50°$; the poor quality of the resulting data is revealed in the relatively high residuals observed in the structure refinement. Details of the crystal data, data collection, and structure refinement are summarized in Table I.

The structure of VIb was solved by direct methods using the SOLV option of SHELXTL,[31] which revealed the locations of the six Co and three P atoms. The remaining non-hydrogen atoms were found in subsequent difference Fourier least-squares re-

Table II. Final Positional and Equivalent Thermal Parameters for VIb

atom	*x*/*a*	*y*/*b*	*z*/*c*	U_{eq}, Å^2
Co(1)	1.0274 (1)	0.2079 (1)	0.4804 (2)	0.037
Co(2)	1.0000 (1)	0.1690 (0)	0.6298 (1)	0.035
Co(3)	0.9180 (1)	0.1687 (1)	0.4759 (2)	0.037
C(1)	1.0213 (7)	0.1576 (3)	0.4905 (9)	0.026
C(2)	1.0609 (7)	0.1302 (3)	0.4442 (9)	0.024
P(1)	1.1358 (2)	0.2241 (1)	0.5316 (3)	0.041
O(111)	1.1462 (6)	0.2335 (3)	0.6471 (8)	0.050
C(111)	1.219 (1)	0.2450 (6)	0.686 (2)	0.083
O(112)	1.2024 (5)	0.1954 (3)	0.520 (1)	0.063
C(112)	1.232 (1)	0.1843 (6)	0.430 (1)	0.084
O(113)	1.1736 (6)	0.2545 (3)	0.4651 (9)	0.073
C(113)	1.132 (1)	0.2885 (4)	0.447 (2)	0.095
C(11)	1.0476 (7)	0.2088 (3)	0.346 (1)	0.029
O(11)	1.0662 (6)	0.2085 (3)	0.2625 (8)	0.059
C(13)	0.9747 (8)	0.2478 (4)	0.510 (1)	0.046
O(13)	0.9424 (7)	0.2725 (3)	0.5259 (9)	0.068
P(2)	0.9417 (2)	0.1264 (1)	0.7063 (3)	0.031
O(211)	0.8562 (6)	0.1307 (3)	0.7102 (8)	0.060
C(211)	0.8100 (8)	0.1053 (5)	0.765 (2)	0.072
O(212)	0.9647 (6)	0.1192 (3)	0.8230 (8)	0.051
C(212)	0.954 (1)	0.1469 (4)	0.903 (1)	0.056
O(213)	0.9508 (6)	0.0869 (3)	0.6670 (8)	0.054
C(213)	1.0227 (9)	0.0706 (4)	0.654 (1)	0.059
C(21)	1.0874 (9)	0.1586 (4)	0.680 (1)	0.039
O(21)	1.1423 (6)	0.1509 (3)	0.7192 (8)	0.054
C(23)	0.9658 (9)	0.2053 (4)	0.706 (1)	0.046
O(23)	0.9472 (6)	0.2288 (3)	0.7569 (9)	0.057
C(31)	0.8863 (8)	0.1232 (4)	0.463 (1)	0.038
O(31)	0.8677 (7)	0.0954 (3)	0.447 (1)	0.074
C(32)	0.8945 (8)	0.1848 (4)	0.349 (1)	0.037
O(32)	0.8767 (6)	0.1935 (3)	0.2692 (8)	0.059
C(33)	0.8488 (9)	0.1907 (4)	0.556 (1)	0.052
O(33)	0.8074 (7)	0.2057 (4)	0.602 (1)	0.081
C(3)	1.0950 (7)	0.1059 (3)	0.3969 (9)	0.027
C(4)	1.1326 (7)	0.0790 (4)	0.347 (1)	0.031
Co(4)	1.1732 (1)	0.0750 (0)	0.2112 (1)	0.028
Co(5)	1.2212 (1)	0.0543 (0)	0.3802 (1)	0.032
Co(6)	1.1015 (1)	0.0312 (0)	0.3137 (1)	0.027
P(4)	1.0888 (2)	0.0823 (1)	0.0965 (3)	0.035
O(411)	1.1102 (5)	0.1081 (2)	0.0023 (7)	0.041
C(411)	1.172 (1)	0.1016 (5)	−0.060 (1)	0.077
O(412)	1.0123 (5)	0.1001 (2)	0.1256 (8)	0.046
C(412)	1.0098 (9)	0.1347 (4)	0.172 (1)	0.053
O(413)	1.0643 (6)	0.0466 (2)	0.0446 (7)	0.046
C(413)	1.007 (1)	0.0468 (4)	−0.033 (1)	0.076
C(41)	1.2086 (8)	0.1194 (4)	0.197 (1)	0.040
O(41)	1.2278 (7)	0.1475 (3)	0.1880 (9)	0.062
C(43)	1.2319 (9)	0.0470 (4)	0.134 (1)	0.043
O(43)	1.2683 (6)	0.0286 (3)	0.0868 (9)	0.060
C(51)	1.2077 (8)	0.0548 (4)	0.518 (1)	0.041
O(51)	1.1981 (6)	0.0567 (3)	0.6048 (9)	0.053
C(52)	1.2919 (9)	0.0873 (4)	0.371 (1)	0.049
O(52)	1.3367 (6)	0.1076 (3)	0.367 (1)	0.087
C(53)	1.2720 (8)	0.0137 (4)	0.354 (1)	0.043
O(53)	1.3028 (7)	−0.0123 (3)	0.3366 (9)	0.072
C(61)	1.0076 (9)	0.0385 (4)	0.286 (1)	0.043
O(61)	0.9442 (6)	0.0430 (3)	0.2722 (8)	0.060
C(62)	1.0901 (9)	0.0078 (4)	0.433 (1)	0.045
O(62)	1.0831 (5)	−0.0075 (3)	0.5094 (9)	0.057
C(63)	1.1259 (7)	−0.0045 (4)	0.223 (1)	0.036
O(63)	1.1385 (6)	−0.0260 (3)	0.1651 (9)	0.055

(29) Worth, G. H. Ph.D. Thesis, University of Otago, 1988.
(30) *International Tables for X-ray Crystallography*; Kynoch Press: Birmingham, England, 1966; Vol. 1.
(31) Sheldrick, G. M. SHELXTL, An Integrated System for Solving, Refining and Displaying Crystal Structures from Diffraction Data; University of Göttingen: Göttingen, Germany, 1980.

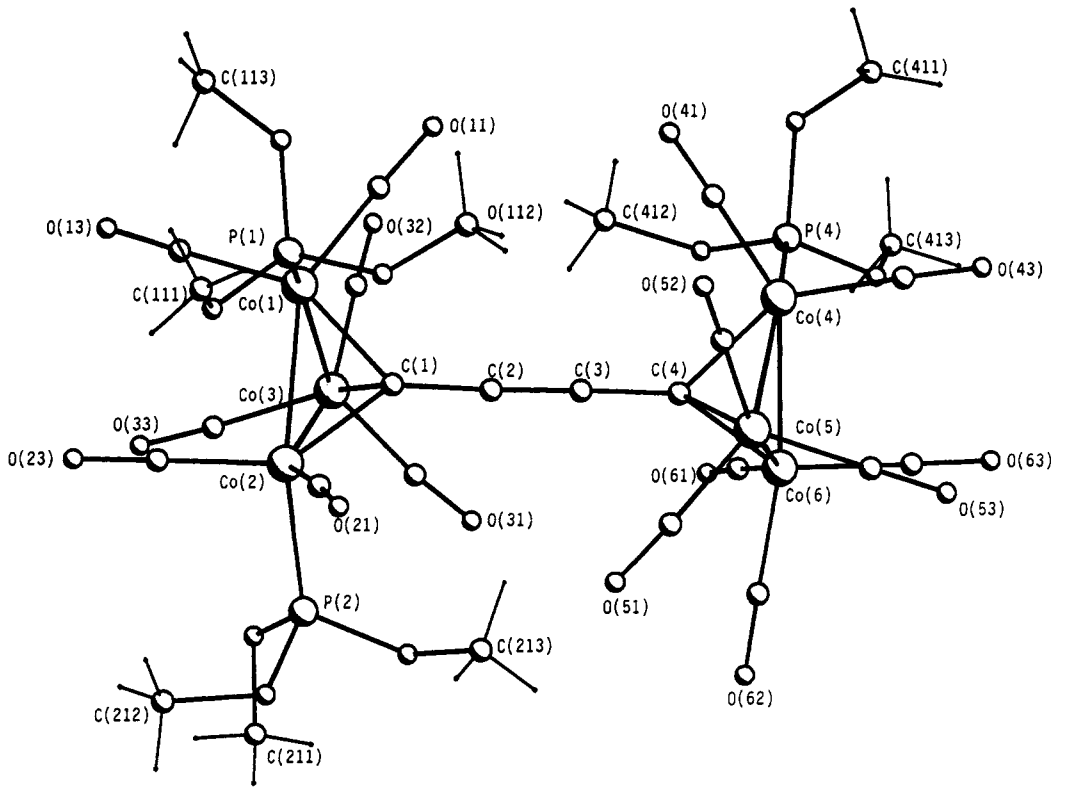

Figure 1. View of molecule VIb.

finement cycles. Refinement minimizing $\sum w(|F_o| - |F_c|)^2$ was performed using SHELX-76.[32] Hydrogen atoms were included in the refinements as fixed contributions to F_c, a weighting scheme was introduced, and the non-hydrogen atoms were refined anisotropically in alternating blocked-matrix cycles. Roughly half of the molecular unit was refined per cycle. Final positional and equivalent thermal parameters for VIb are given in Table II.

Results

Synthesis. Preparations for the monoalkyne derivatives I and alkyne-linked clusters II are described elsewhere.[15] Attempts to improve on the previous serendipitous syntheses of III–V met with little success. Alkyne cleavage is a well-trodden route[33,34] to clusters containing "carbyne" carbon atoms, and while thermolysis under argon or in vacuo of alkyne complexes did give CCo_3 derivatives, yields are less than 5%. However, the Lewis-base-assisted reductive coupling and removal of bromide from $BrCCo_3(CO)_9$ to give III[19] was modified to give >30% yields of III or, in the presence of CO, >60% yields of IV:

$$2BrCCo_3(CO)_9 + Ph_3As \rightarrow (CO)_9Co_3C\text{–}CCo_3(CO)_9 + Ph_3AsBr_2 \quad (1)$$

$$CO + 2BrCCo_3(CO)_9 + Ph_3As \rightarrow (CO)_9Co_3C\text{–}C(O)\text{–}CCo_3(CO)_9 + Ph_3AsBr_2 \quad (2)$$

Improved structural data for IV were obtained by a low-temperature X-ray determination and are described elsewhere.[34]

The strategy adopted to give clusters analogous to II and III, but with nonequivalent cluster redox sites, was to synthesize Lewis-base derivatives. Surprisingly, we were unable to characterize derivatives of III; spectroscopic monitoring of the reactions indicated that complexes with one or two PR_3 or $P(OR)_3$ substituents per cluster unit had a transient existence but they decomposed on workup. Models indicate that the intramolecular interactions in derivatives of III, where the Lewis base is coordinated in the usual equatorial site, would be considerable and the instability of these complexes is attributed to this factor. In contrast, separation of the two cluster units as in II relieves the steric strain and a number of derivatives VI were isolated (eq 3); one with L = $P(OMe)_3$ (n = 1, m = 2; VIb) was structurally characterized.

$$(CO)_9Co_3CC{\equiv}CCo_3(CO)_9 + (m+n)L \rightarrow L_m(CO)_{9-m}Co_3CC{\equiv}CCo_3(CO)_{9-n}L_n \quad (3)$$

n = 0, 1; m = 0, 1; L = PPh_3, $P(OMe)_3$

n = 1, 2; m = 1, 3; L = $P(OMe)_3$

Structural Characterization of VIb. As in the crystal structure of the parent compound $C_2[CCo_3(CO)_9]_2$[22] the unit cell of VIb consists of well-separated molecules of $C_4Co_6(CO)_{15}[(MeO)_3P]_3$, no intermolecular contact (excluding H atoms) being closer than 3.0 Å. A view of the molecule perpendicular to the plane of one of the Co_3 triangles is shown in Figure 1, with selected angle and bond length data in Table III. The two alkyne-linked $CCo_3(CO)_9$ units have respectively one or two equatorially coordinated phosphite ligands. The remaining carbonyl groups on those Co atoms are terminal and are arranged one equatorially and the other axially such that the Co atoms have a distorted-octahedral environment. Two CCo_3 units are linked via a C≡C bridge so that the central part of the molecule consists of a linear CC≡CC chain, little different from that of the unsubstituted parent,[22] and the bond lengths C(1)–C(2) = 1.39 (2) Å, C(2)–C(3) = 1.26 (2) Å, and C(3)–C(4) = 1.38 (2) Å are indicative of π-electron-density dispersion between the triple bond and both cluster units. There is a nonuniform arrangement of the ligands about each cobalt, which minimizes the interaction

(32) Sheldrick, G. M. SHELX-76, Program for Crystal Structure Determination; University of Cambridge, Cambridge, U.K., 1976.
(33) Freeland, B. H.; Hux, J. E.; Nicholas, C. P.; Kenneth, G. T. *Inorg. Chem.* **1980**, *19*, 693. Schilling, B. E. R.; Hoffmann, R. J. *Acta Chem. Scand.* **1979**, *B33*, 231.
(34) Worth, G. H.; Robinson, B. H.; Simpson, J. Submitted for publication in *Acta Crystallogr.*
(35) Colbran, S. B.; Robinson, B. H.; Simpson, J. *Organometallics* **1983**, *2*, 943.

Table III. Selected Bond Lengths and Angles for VIb

Bond Lengths (Å)			
Co(1)–Co(2)	2.470 (3)	C(3)–C(4)	1.38 (2)
Co(1)–Co(3)	2.467 (3)	C(4)–Co(4)	1.91 (1)
Co(1)–C(1)	1.90 (1)	C(4)–Co(5)	1.90 (1)
Co(1)–P(1)	2.155 (4)	C(4)–Co(6)	1.93 (1)
Co(1)–C(11)	1.78 (2)	Co(4)–Co(5)	2.474 (3)
Co(1)–C(13)	1.82 (2)	Co(4)–Co(6)	2.476 (2)
Co(2)–Co(3)	2.480 (3)	Co(4)–P(4)	2.144 (4)
Co(2)–C(1)	1.89 (1)	Co(4)–C(41)	1.79 (2)
Co(2)–P(2)	2.155 (4)	Co(4)–C(43)	1.79 (2)
Co(2)–C(21)	1.75 (2)	Co(5)–Co(6)	2.483 (3)
Co(2)–C(23)	1.79 (2)	Co(5)–C(51)	1.80 (2)
Co(3)–C(1)	1.92 (1)	Co(5)–C(52)	1.78 (2)
Co(3)–C(31)	1.81 (2)	Co(5)–C(53)	1.81 (2)
Co(3)–C(32)	1.80 (2)	Co(6)–C(61)	1.76 (2)
Co(3)–C(33)	1.82 (2)	Co(6)–C(62)	1.79 (2)
C(1)–C(2)	1.39 (2)	Co(6)–C(63)	1.84 (2)
C(2)–C(3)	1.26 (2)		

Bond Angles (deg)			
Co(2)–Co(1)–Co(3)	60.3 (1)	C(3)–C(4)–Co(4)	132 (1)
Co(2)–Co(1)–C(1)	49.2 (4)	C(3)–C(4)–Co(5)	132 (1)
Co(2)–Co(1)–P(1)	96.3 (1)	C(3)–C(4)–Co(6)	130 (1)
Co(2)–Co(1)–C(11)	144.8 (4)	Co(4)–C(4)–Co(5)	81.0 (5)
Co(2)–Co(1)–C(13)	102.6 (5)	Co(4)–C(4)–Co(6)	80.3 (5)
Co(3)–Co(1)–C(1)	50.2 (4)	Co(5)–C(4)–Co(6)	80.9 (5)
Co(3)–Co(1)–P(1)	154.7 (2)	C(4)–Co(4)–Co(5)	49.3 (4)
Co(3)–Co(1)–C(11)	98.8 (4)	C(4)–Co(4)–Co(6)	50.2 (4)
Co(3)–Co(1)–C(13)	94.4 (5)	C(4)–Co(4)–P(4)	110.6 (4)
C(1)–Co(1)–P(1)	108.2 (4)	C(4)–Co(4)–C(41)	99.2 (6)
C(1)–Co(1)–C(11)	95.6 (6)	C(4)–Co(4)–C(43)	141.5 (6)
C(1)–Co(1)–C(13)	141.0 (6)	Co(5)–Co(4)–Co(6)	60.2 (1)
Co(1)–Co(2)–Co(3)	59.8 (1)	Co(5)–Co(4)–P(4)	154.1 (1)
Co(1)–Co(2)–C(1)	49.3 (4)	Co(5)–Co(4)–C(41)	105.0 (4)
Co(1)–Co(2)–P(2)	153.5 (1)	Co(5)–Co(4)–C(43)	95.6 (5)
Co(1)–Co(2)–C(21)	104.0 (5)	Co(6)–Co(4)–P(4)	94.7 (1)
Co(1)–Co(2)–C(23)	92.7 (5)	Co(6)–Co(4)–C(41)	149.2 (5)
Co(3)–Co(2)–C(1)	50.0 (4)	Co(6)–Co(4)–C(43)	102.5 (5)
Co(3)–Co(2)–P(2)	94.1 (1)	C(4)–Co(5)–Co(4)	49.7 (4)
Co(3)–Co(2)–C(21)	146.6 (5)	C(4)–Co(5)–Co(6)	50.1 (4)
Co(3)–Co(2)–C(23)	103.7 (5)	C(4)–Co(5)–C(51)	95.9 (6)
C(1)–Co(2)–P(2)	111.6 (4)	C(4)–Co(5)–C(52)	104.6 (6)
C(1)–Co(2)–C(21)	96.9 (6)	C(4)–Co(5)–C(53)	142.9 (6)
C(1)–Co(2)–C(23)	139.8 (6)	Co(4)–Co(5)–Co(6)	59.9 (1)
Co(1)–Co(3)–Co(2)	59.9 (1)	Co(4)–Co(5)–C(51)	145.5 (5)
Co(1)–Co(3)–C(1)	49.3 (4)	Co(4)–Co(5)–C(52)	88.7 (6)
Co(1)–Co(3)–C(31)	145.1 (5)	Co(4)–Co(5)–C(53)	106.2 (5)
Co(1)–Co(3)–C(32)	90.6 (5)	Co(6)–Co(5)–C(51)	103.2 (5)
Co(1)–Co(3)–C(33)	105.5 (5)	Co(6)–Co(5)–C(52)	147.6 (5)
Co(2)–Co(3)–C(1)	48.9 (4)	Co(6)–Co(5)–C(53)	94.8 (5)
Co(2)–Co(3)–C(31)	105.5 (5)	C(51)–Co(5)–C(52)	98.9 (7)
Co(2)–Co(3)–C(32)	150.5 (5)	C(51)–Co(5)–C(53)	105.0 (7)
Co(2)–Co(3)–C(33)	87.4 (6)	C(52)–Co(5)–C(53)	102.1 (7)
C(1)–Co(3)–C(31)	96.5 (6)	C(4)–Co(6)–Co(4)	49.5 (4)
C(1)–Co(3)–C(32)	113.0 (6)	C(4)–Co(6)–Co(5)	49.0 (4)
C(1)–Co(3)–C(33)	135.3 (7)	C(4)–Co(6)–C(61)	100.5 (6)
Co(1)–C(1)–Co(2)	81.5 (5)	C(4)–Co(6)–C(62)	107.3 (6)
Co(1)–C(1)–Co(3)	80.5 (5)	C(4)–Co(6)–C(63)	138.9 (6)
Co(1)–C(1)–C(2)	132 (1)	Co(4)–Co(6)–Co(5)	59.9 (1)
Co(2)–C(1)–Co(3)	81.2 (5)	Co(4)–Co(6)–C(61)	107.0 (5)
Co(2)–C(1)–C(2)	133 (1)	Co(4)–Co(6)–C(62)	148.0 (5)
Co(3)–C(1)–C(2)	128 (1)	Co(4)–Co(6)–C(63)	91.0 (4)
C(1)–C(2)–C(3)	176 (1)	Co(5)–Co(6)–C(61)	149.2 (5)
C(2)–C(3)–C(4)	178 (1)	Co(5)–Co(6)–C(62)	88.5 (5)
		Co(5)–Co(6)–C(63)	105.5 (4)

between the phosphite groups and apical group and with the carbonyl ligands. This is particularly evident in the broad range of values for the bond angles C_{apical}–Co–L_{eq} (C_{eq} 95.6 (6)–113.0 (6)°; P, 108.2 (4)–111.6 (4)°) and C_{apical}–Co–C_{ax} (135.3 (7)–142.9 (6)°) (Table I). The mean value for the C_{apical}–Co–C_{eq} angles in $C_2[CCo_3(CO)_9]_2$ is 103.3 (3)°, indicating that substitution by phosphite causes most of the equatorial carbonyls to be bent toward the apical group, while the phosphite groups are bent away. In addition, the two CCo_3 units are staggered in such way as to minimize the interaction between the phosphite ligands on the two centers. The parameters for the phosphite coordination sphere do not differ significantly from those observed for $MeCCo_3(CO)_6[(MeO)_3P]_3$,[28] and there is no evidence that major perturbations of either the cluster skeleton or the bridging alkyne moiety result from phosphite coordination.

Redox Chemistry. Electrochemical data are given in Table IV. Assignments for the various electrode processes are based on data for known couples; thus, an isolated $CCo_3(CO)_9$ unit should be reduced at potentials in the range −0.4 to −0.7 V in CH_2Cl_2 vs Ag/AgCl[11,27,36] and $Co_2(CO)_6$ groups bound to an alkyne in the range −0.65 to −1.10 V.[37] The transient electrochemistry of molecules of type I will be discussed first, as they provide a backdrop for the more complicated redox behavior of molecules with two clusters linked by carbon–carbon bonds. The electrochemical responses of $PhC_2CCo_3(CO)_9$ (Ie) are complex because of its facile transformation to the cyclopentadienone derivative $Ph_2[CCo_3(CO)_9]_2C_4(CO)$[37] during the electrochemical investigations and will not be considered in this paper.

Electrochemistry of Complexes with One $CCo_3(CO)_9$ Entity. (a) $FcC_2CCo_3(CO)_9$ (Ic). Both an oxidizable (ferrocenyl) and a reducible center (cluster) are present in molecule Ic, and most importantly, the ferrocenyl redox center provides an internal standard for the electron-transfer processes without complications due to widely differing diffusion coefficients for ferrocene (as an external reference) and clusters.[27,38]

A chemically reversible oxidation in the cyclic voltammograms (Figure 2), $E_{1/2}^{1+/0} = 0.84$ V and $i_p^c/i_p^a = 1$, can be assigned to the ferrocenyl couple. In common with all these large clusters the electron transfer was slow and the E_p^c/E_p^a separation was large (140 mV on Pt) for a one-electron transfer despite attempts to minimize resistance effects by standard electrochemical techniques[30] (a Nernstian separation of 59 mV for the one-electron reduction of $PhCCo_3(CO)_9$ was readily achieved in CH_2Cl_2 under the same experimental conditions). Slightly better electrode kinetics for Ic were obtained on glassy-carbon electrodes, but since these electrodes were unsuitable for some clusters, all data in this paper will refer to electron transfer at Pt electrodes.

The companion reduction wave at $E_{1/2} = -0.48$ V is chemically reversible but not electrochemically reversible over the temperature range 204–293 K ($i_p^a/i_p^c = 1$) and is clearly a one-electron-reduction process ($\Delta E = 150$ mV, $i_p^a(Fc)/i_p^c$ (reduction) = 1) centered on the $(CO)_9Co_3C$ moiety. A further irreversible reduction process at $E_p^c = -1.25$ V is assigned to the formation of the dianion, which rapidly fragments, as evidenced by the wave at 0.35 V due to the oxidation of $Co(CO)_4^-$.

In summary, the electron-transfer processes for Ic are an uncomplicated superposition of the two individual redox centers:

$$Fc^+C_2CCo_3(CO)_9 \xrightarrow{e^-} FcC_2CCo_3(CO)_9 \xrightarrow{e^-}$$

$$FcC_2CCo_3(CO)_9^- \xrightarrow{e^-} FcC_2CCo_3(CO)_9^{2-} \quad (4)$$

(b) $Me_3SiC_nCCo_3(CO)_9$ (n = 2, 4; Ia,b). Both compounds Ia and Ib display a chemically reversible reduction

(36) Arewgoda, C. M.; Rieger, P. H.; Robinson, B. H.; Simpson, J.; Visco, S. *J. Am. Chem. Soc.* **1982**, *104*, 5633.
(37) Worth, G. H.; Robinson, B. H.; Simpson, J. *J. Organomet. Chem.* **1990**, *387*, 337.
(38) Downard, A. J. Ph.D. Thesis, University of Otago, 1985, and unpublished work.
(39) Geiger, W. E. *Prog. Inorg. Chem.* **1985**, *33*, 275.
(40) Bard, A. J.; Faulkner, A. R. *Electrochemical Methods: Fundamentals and Applications*; Wiley: New York, 1980.

Table IV. Electrochemical Data for $RCCo_3(CO)_9$[a]

R	redn 1[b] $E_{1/2}$[c]	redn 1 $E_{1/4} - E_{3/4}$[c]	redn 1 E_p^c	redn 1 E_p^a	redn 1 i_p^a/i_p^c	redn 2 $E_{1/2}$	redn 2 E_p^c	redn 2 E_p^a	redn 2 i_p^a/i_p^c
Ph	−0.56	60	−0.59	−0.53	1				
PhC_2	−0.45	80	−0.58	−0.40	0.8				
Me_3SiC_2	−0.39	70	−0.49	−0.35	1				
Me_3SiC_4	−0.39	70	−0.44	−0.34	1				
FcC_2[d]	−0.48	60	−0.62	−0.47	1	−0.93	−1.24		
$CCo_3(CO)_9$	−0.41	60	−0.51	−0.41	1	−0.77	−0.85	−0.75	1
$C(O)CCo_3(CO)_9$	−0.36	60	−0.43	−0.29	1	−0.64	−0.66	−0.53	1
$C_2CCo_3(CO)_9$	−0.40	60	−0.48	−0.32	1	−0.60	−0.68	−0.51	1
$C_4CCo_3(CO)_9$			−0.48	−0.30	1		−0.58	−0.40	0.9

[a] In CH_2Cl_2 vs Ag/AgCl, 0.1 M $Bu_4N^+PF_6^-$ at 293 K; CV scan rate 200 mV s^{-1}. [b] For $CCo_3(CO)_9$ redox center. [c] Drop time 0.5 s at 10 mV s^{-1}; $E_{1/2}$ in V, $E_{1/4} - E_{3/4}$ in mV. [d] $E_{1/2}$ for $[Fc]^{+/-}$ couple is 0.84 V.

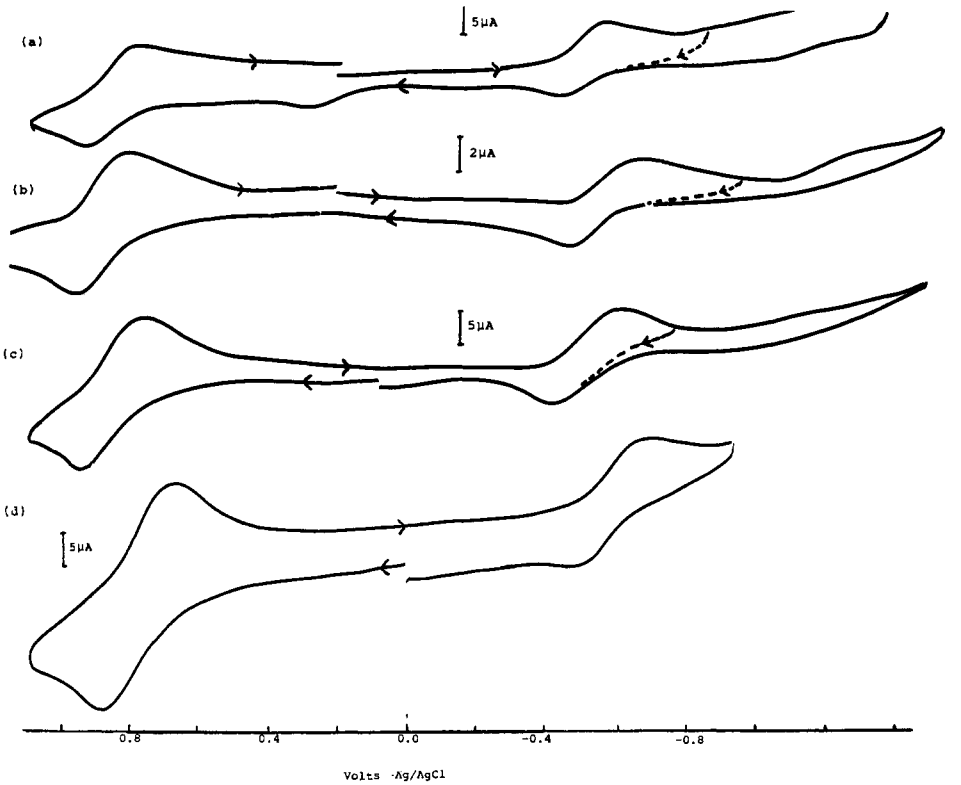

Figure 2. Cyclic voltammogram of Ic at Pt in CH_2Cl_2 under Ar (V vs Ag/AgCl; 0.1 M Bu_4NPF_6 (TBAF)): (a) scan rate 200 mV s^{-1}, 293 K; (b) scan rate 200 mV s^{-1}, 204 K; (c) scan rate 50 mV s^{-1}, 293 K; (d) scan rate 1 V s^{-1}, 293 K.

process (−0.43 and −0.49 V, respectively) followed by the irreversible formation of a dianion at ~1.3 V (Figure 3). The diffusion currents for the first reduction waves were approximately 60% of that for equimolar ferrocene added to the electrochemical solution. When compensated for the relative diffusion coefficient for ferrocene (2.0×10^{-5} cm^2 s^{-1}) compared with that for $PhCCo_3(CO)_9$ (9.8×10^{-6} cm^2 s^{-1}), these data, together with $\Delta E \approx 140$ mV, are indicative of a slow one-electron transfer to give a radical anion with the unpaired electron centered on the CCo_3 core (eq 5; the assumption that the diffusion coefficients for $PhCCo_3(CO)_9$ and Ia,b are similar is not unreasonable in our view and is borne out by data for other $RCCo_3(CO)_9$ clusters,[38] for example ($\times 10^{-6}$ cm^2 s^{-1}) R = Me (8.3), Me_3Si (8.6)).

$$Me_3Si{-}C{\equiv}C{-}C{\equiv}C{-}CCo_3(CO)_9 \underset{-e}{\overset{+e}{\rightleftharpoons}} Me_3Si{-}C{\equiv}C{-}C{\equiv}C{-}CCo_3(CO)_9^{\bullet}$$

I(b)

$$\xrightarrow{+e} Me_3Si{-}C{\equiv}C{-}C{\equiv}C{-}CCo_3(CO)_9^{2-} \qquad (5)$$

(c) Lewis Base Derivatives. Phosphine and phosphite derivatives $Me_3SiC_2CCo_3(CO)_8L$ and $FcC_2CCo_3(CO)_8L$ show electrochemical behavior identical with that of other Lewis base derivatives of the tricobalt carbon cluster.[12] Formation of the radical anions occurs at potentials within the range previously observed, and radical anion formation is followed by the complex $\vec{E}c\vec{E}$ processes described elsewhere.[12,41]

Electrochemistry of Molecules with Two $CCo_3(CO)_9$ Clusters. From the results just described, one could predict that molecules with two noninteracting $CCo_3(CO)_9$ entities would display transient current/voltage traces consisting of a single reduction wave but with twice the diffusion current relative to that of molecules with only one cluster. On the other hand, clusters that were interacting in an electrochemical sense would display two reversible couples with a potential separation determined by the extent of the interaction.[39,40,42]

(a) $[CCo_3(CO)_9]_2$ (III). Molecule III is unusual in the sense that it is one of the few examples of two unfettered metal carbonyl clusters being directly linked by a carbon–carbon bond. As such, it is a prime candidate for an

(41) Hinkelmann, K.; Heinze, J.; Schecht, H.-T.; Field, J. S.; Vahrenkamp, H. *J. Am. Chem. Soc.* **1989**, *111*, 5078.
(42) Flanagan, J. B.; Margel, S.; Bard, A. J.; Anson, F. C. *J. Am. Chem. Soc.* **1978**, *100*, 4248.

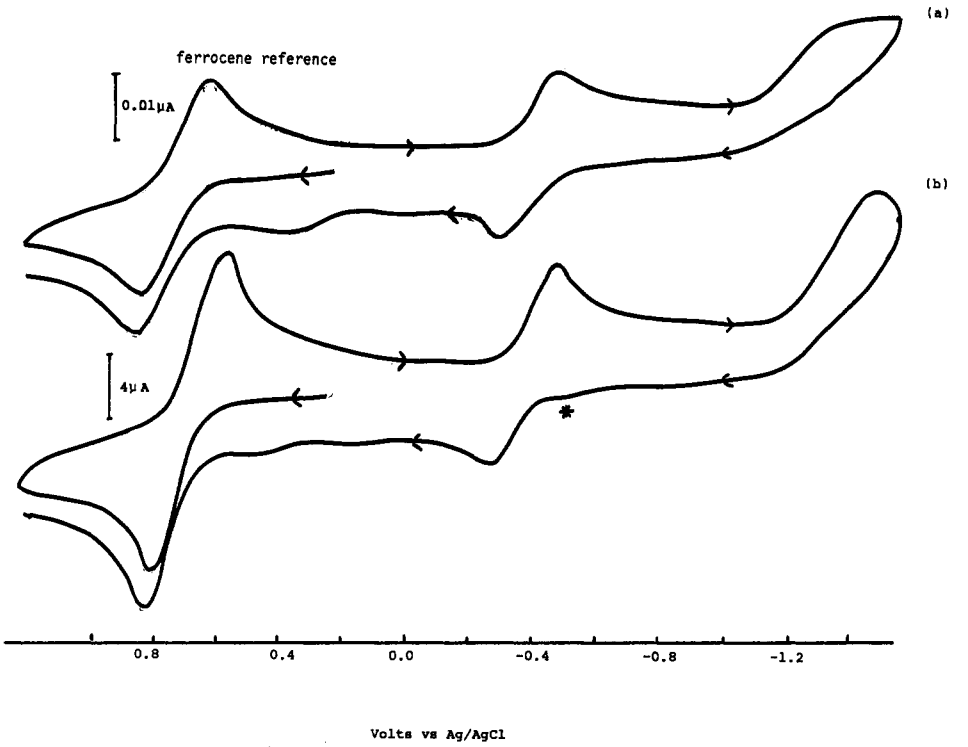

Figure 3. Cyclic voltammograms of Ib at Pt in CH_2Cl_2 under Ar (0.1 M TBAF; equimolar in situ ferrocene as reference): (a) scan rate 100 mV s^{-1}, 293 K; (b) scan rate 500 mV s^{-1}, 204 K.

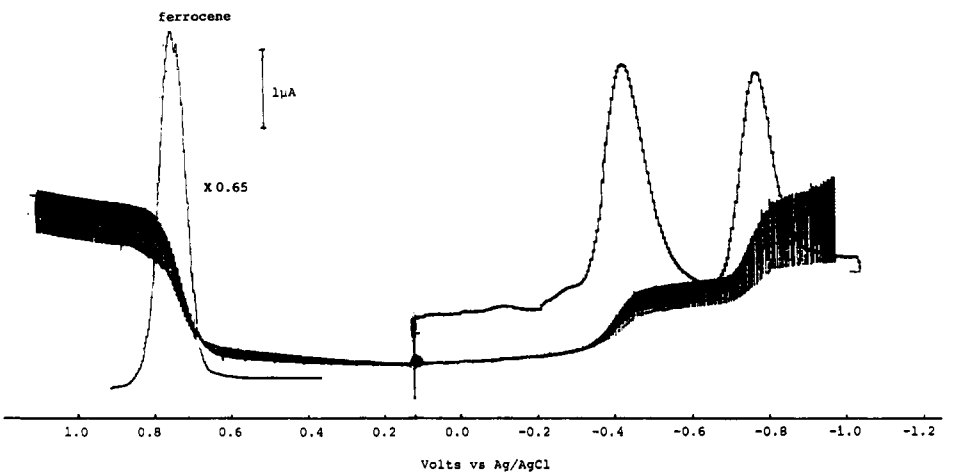

Figure 4. Differential pulse and dc polarogram for III in CH_2Cl_2 at 293 K on Hg (drop time 0.5 s, scan rate 10 mV s^{-1}; 0.1 M TBAF; equimolar in situ ferrocene as reference).

investigation of electronic interactions between two capped clusters, particularly as the carbon–carbon bond linkage at 134 pm is consistent with a partial π component.[22] This bond length must also be seen in the context of the extensive nonbonded repulsive interactions between the equatorial CO groups which will tend to lengthen, rather than shorten, the link.

Differential pulse and dc polarograms of III at 293 K display *two* reduction waves at $E_{1/2}(1) = -0.41$ V and $E_{1/2}(2) = -0.77$ V with a current ratio of approximately 0.9 (Figure 4). The first has the characteristics of an electrochemically reversible one-electron transfer (Table IV), but the second has an $E_{1/4} - E_{3/4}$ separation of 50 mV. Both waves have a dependence on drop time, suggesting that there is an associated fast chemical process.

At low temperatures cyclic voltammograms of III are simple, with *two* apparently chemically reversible one-electron-transfer steps (Figure 5a). Currents relative to the in situ ferrocene couple are appropriate for one-electron processes, given the difference in diffusion coefficients between the cluster and ferrocene. An analysis of these quasi-reversible responses gives $E_{1/2}(A) = -0.41$ V and $E_{1/2}(B) = -0.77$ V, indicating that mercury is not interfering in the polarographic experiments. However, as the temperature increases, both waves progressively become less reversible with the concomitant appearance of a third electron-transfer process ($E_{1/2}(C) = \sim 0.1$ V) at potential *positive* of A. The relationship between the three processes is readily seen from Figure 5b. Couple C is derived from the first radical anion, as it does not appear on the initial reduction scan but appears on the reverse scan if the switching potential is >−0.50 V. The new couple (C) is nearly chemically reversible at fast scan rates (>200 mV s^{-1}) (as is A) with the characteristic of a one-electron wave; at slow scan rates both couples A and C have $i_p^a/i_p^c < 1$. Similarly, both couples are only partly chemically reversible if the switching potential is negative of the cathodic component of couple B and an oxidation process due to $Co(CO)_4^-$ appears on all scans. Cathodic peak potentials for A decrease with increasing scan rates, as expected for

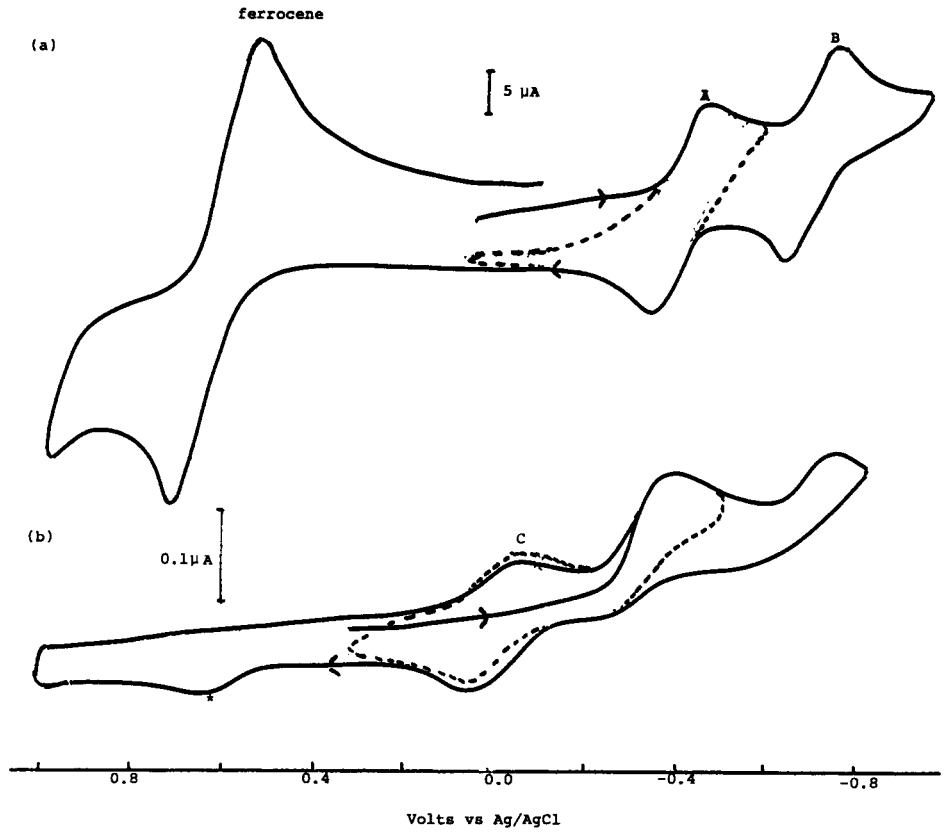

Figure 5. Cyclic voltammograms for III in CH_2Cl_2 (0.1 M TBAF under Ar; dotted lines are repeat scans at different switching potentials): (a) scan rate 500 mV s^{-1}, 223 K, equimolar in situ ferrocene for reference; (b) scan rate 500 mV s^{-1}, 293 K.

a couple involved in an $\tilde{E}C$ mechanism ($\Delta E_p/\log v = 29$ mV), while $I^p_c/v^{1/2}$ varies with scan rate, behavior typical of an $\tilde{E}C\tilde{E}$ process. Adsorption at the electrode surface can produce apparently reversible prewaves if the product of the first reduction step is strongly adsorbed onto the electrode surface.[40] We do not believe that C is due to interfacial phenomena for two reasons. First, the profile of the new couple C was not typical of an adsorption wave, as it displayed a $v^{1/2}$ scan rate dependence, and second, the same voltammetric responses were obtained at a glassy-carbon electrode and in other solvents. Consequently the new species IIIZ must be derived from a slow chemical reaction involving the first reduction product $III^{\bullet-}$ but the formation of IIIZ does not involve fragmentation of the cluster as it is converted into III. This explains why couple B is not chemically reversible other than at low temperatures. Schematically the overall electrode processes are therefore as shown in eq 6. This is a typical

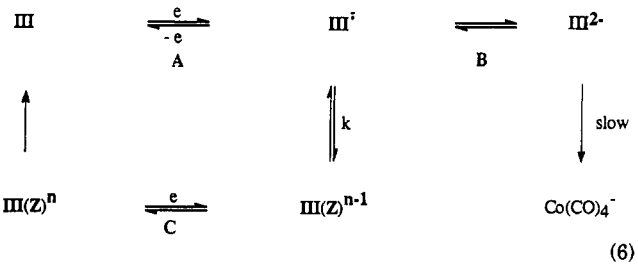

(6)

ECEC or "square" scheme with the chemical reactions discrete from the charge transfer. A precise treatment of the kinetic regime is difficult because the voltammetric response is influenced by the rate of chemical reaction and quasi-reversible charge transfer; an estimate for the first-order rate constant k_1 for the conversion to IIIZ is 10^{-3} s^{-1}. Identification of the new species is discussed below, but the most important electrochemical fact is that the

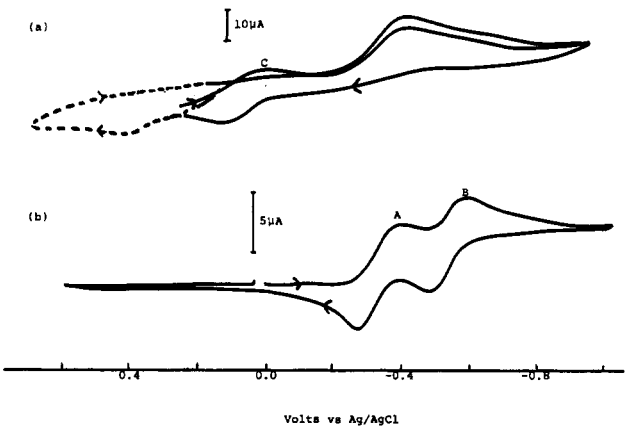

Figure 6. Cyclic voltammograms for IV at Pt in CH_2Cl_2 under Ar (0.1 M TBAF under Ar): (a) scan rate 200 mV s^{-1}, 293 K, dotted line is repeat scan not switched at 0.2 V; (b) scan rate 100 mV s^{-1}, 223 K.

first reduction process involves a transfer of *one electron* despite the two redox centers being identical. Therefore, *the two redox centers are coupled* from an electrochemical, and presumably electronic, perspective.[39,42]

(b) Electrochemistry of $(CO)_9Co_3C(CO)CCo_3(CO)_9$ (IV). In this molecule there is a much greater separation between the two equatorial sets of CO groups and this provided a check on whether the coupling of the two redox centers in III was via "through-space" interactions. In fact, the electrochemistry of IV is very similar to that of III. Thus, at 223 K two chemically reversible waves are found in the cyclic voltammograms (Figure 6b) but as the temperature is increased a new reversible couple appears at $E_{1/2} \approx 0.0$ V; the first initial reduction reduction process tends to become irreversible while the second reduction wave at $E_{1/2} = -0.77$ V is lost (Figure 6a). Obviously the

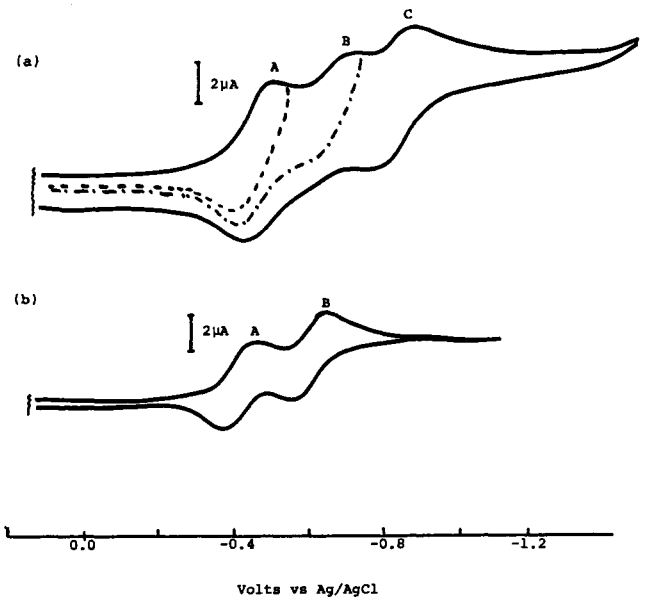

Figure 7. Cyclic voltammograms for IIa at Pt in CH_2Cl_2 under Ar: (a) scan rate 200 mV s^{-1}, 293 K; (b) scan rate 200 mV s^{-1}, 243 K.

same explanation as given above for III can be advanced with the proviso that the chemical reaction is much faster for $IV^{\bullet-}$.

(c) Electrochemistry of $(CO)_9Co_3CC{\equiv}CCCo_3(CO)_9$ (IIa). Mechanistically, the same redox pattern observed in the archetypical III is followed but with a marked change in the potential of the third couple. In this molecule the two redox centers are 4.43 Å apart but the alkyne group could provide the electronic bridge between clusters.

Low-temperature responses display two chemically reversible one-electron couples at $E_{1/2}$ = −0.39 V (A) and −0.60 V (B), respectively (Figure 7b). Above 243 K a new couple is observed (Figure 7a) at a potential *negative* of the second couple. This couple is apparently chemically reversible at all scan rates, as is the first couple A; i_p^c(C) decreases with increasing scan rate in tandem with a corresponding increase in i_p^c(B) (precise measurements are difficult because of the small differences in E_p^c).

(d) Electrochemistry of Other Molecules with Two Linked $CCo_3(CO)_9$ Clusters. At low temperatures the transient electrochemistry of IIb was very similar in profile to that of IIa except that a small difference between potential $E_{1/2}$(A) and $E_{1/2}$(B) made it difficult to unravel the kinetic relationships of the current/voltage responses.

Significantly, when one triple bond of IIb was effectively removed as a member of a delocalized diacetylene bridge by coordination to a $Co_2(CO)_6$ entity (i.e. molecule V), there was no evidence for the formation of couple C. The current due to the couple $[CCo_3(CO)_9]^{0/-}$ was *twice* that of $[C_2Co_2(CO)_6]^{0/-}$, as expected if the two cluster units were acting independently (although strictly they are structurally nonequivalent).

(e) Bulk Chemical and Electrochemical Reduction of IIa, III, and IV in Solution. To assist in the structural characterization of the reduced species, a spectroscopic investigation was carried out on solutions of III reduced by electrochemical or chemical methods.

Exhaustive reduction of a CH_2Cl_2 solution of III at potentials negative of the second redox process for this molecule produced a dark brown solution. Cyclic voltammetry confirmed that none of III remained and that a reduced species of a new cluster, responsible for the reversible couple C seen in the transient electrochemistry, was the only cluster product. Coulometry for the reduction step gave approximately 1.30 ± 0.07 mol of electrons transferred per mole of III at −0.55 V and 1.70 ± 0.2 mol of electrons at −0.66 V (the values increase with potential and the increasing amount of $Co(CO)_4^-$ being formed). Oxidation of these reduced solutions at potentials >0.6 V re-formed III quantitatively after allowance is made for the cobalt content of the $Co_2(CO)_8$ produced as a decomposition product. However, *oxidation at* 0.2 V and at 273 K did not *initially* yield III; rather, oxidation of the reduced IIIZ cluster occurred with the overall transfer of *1* mol of electrons. The lifetime of this oxidized species in the electrochemical solutions at 273 K is extemely short, with conversion to III occurring virtually as it is produced. Concurrent IR studies during the electrochemical reduction confirmed that a reduced carbonyl species, $IIIZ^{\bullet-}$ (ν(CO) 1995, 1975 cm^{-1} (terminal carbonyl) and 1773 cm^{-1} (bridging)), was the ultimate cluster product (Figure 8).

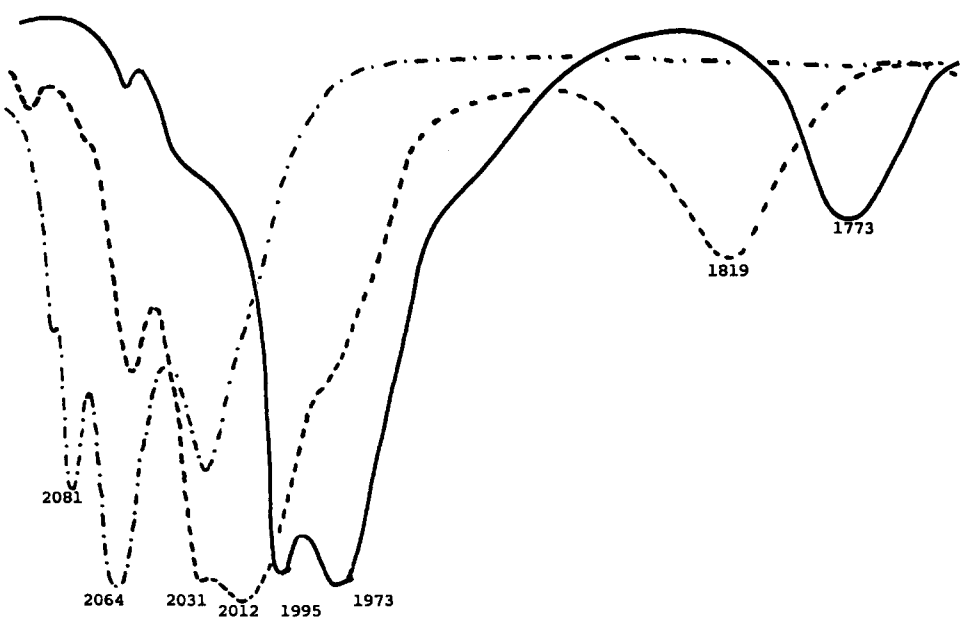

Figure 8. Infrared spectra in CH_2Cl_2 of species obtained by electrochemical reduction of III and oxidation of the reduction products under Ar at 293 K: (—) reduction of III at V; (- - -) oxidation of reduced species Z at 0.8 V; (–·–) oxidation of reduced species $IIIZ^{\bullet-}$ at 0.2 V.

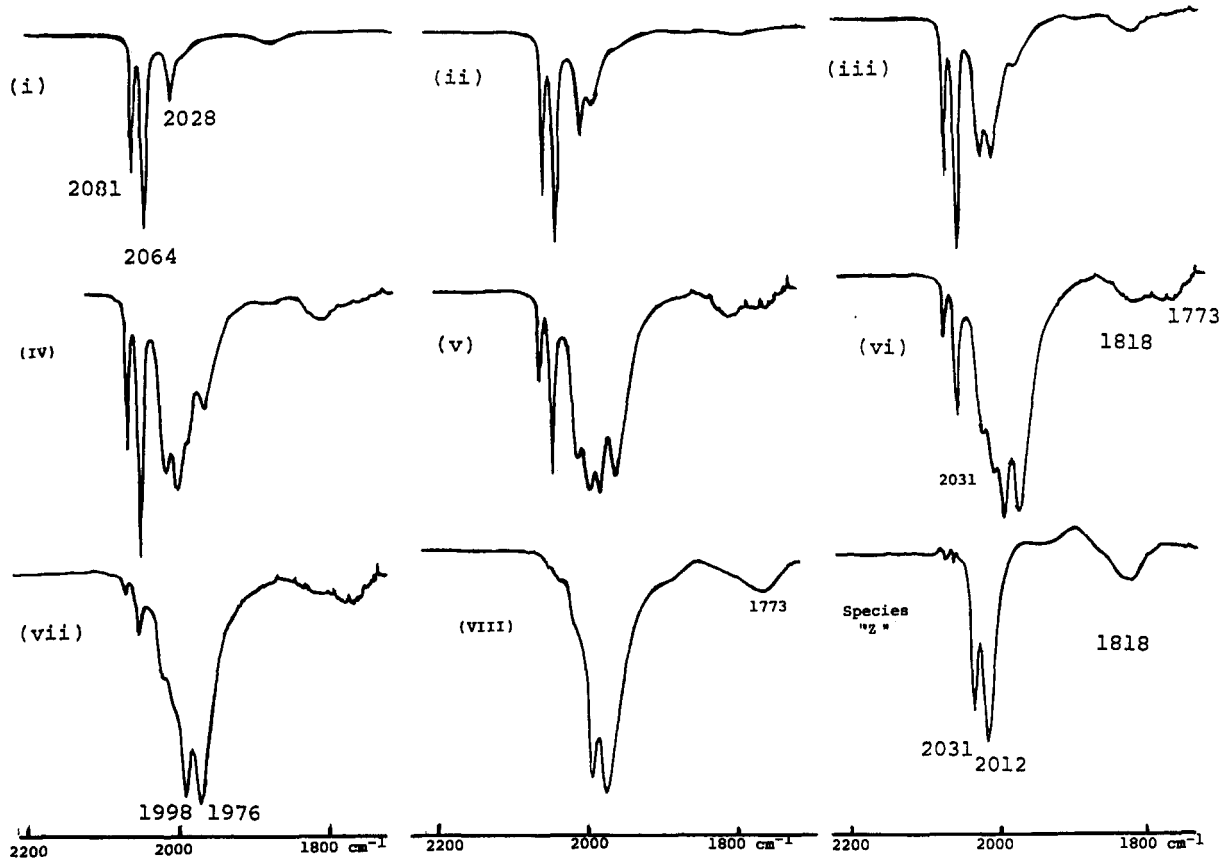

Figure 9. Sequential infrared spectra during the reduction of III by cobaltocene in CH_2Cl_2 under Ar.

Oxidation at 0.2 V shifted these bands to 2025, 2013 and 1819 cm^{-1}, respectively (Figure 8); this spectrum is attributed to the oxidized species of couple C, IIIZ.

Chemical reduction of III by 1.1 ± 0.2 mol equiv of cobaltocene gave a quantitative yield of $IIIZ^{\bullet-}$ with a ν(CO) spectrum identical with that of the product formed by exhaustive electrolysis (Figure 9). This gives confidence in the electrochemical results. More subtle changes in the structure of the reduced intermediates were discernible from the sequential chemical reduction (Figure 9). An intermediate with a spectrum similar to that of the species IIIZ noted above (ν(CO) 2031, 2012, and 1818 cm^{-1}) was identified, and a detailed analysis of the spectra in Figure 9 confirms that the sequence is explicable on the basis of only three species, III, $IIIZ^{\bullet-}$, and IIIZ. No ESR spectrum, either in solution or as a glass, was detected in the temperature range 20–293 K for any of the reduced species. Likewise, no bands were found in the near-IR spectra of the reduced solutions down to 260 K—precipitation occurred below this temperature in CH_2Cl_2—these would be anticipated for a mixed-valence species. Attempts to crystallize $IIIZ^{\bullet-}$ using a variety of counterions were unsuccessful, but the isolated solids had the same ν(CO) bands as those assigned above to this radical anion.

Cobaltocene and electrochemical reductions of IIa and IV were bedeviled by the large amounts of $Co(CO)_4^-$ produced in solution. Nevertheless, cobaltocene reduction of IV gave a single unstable product species (ν(CO) 2005, 1984, 1790 cm^{-1}) with a spectral profile similar to that of $IIIZ^{\bullet-}$; evidence for the intermediate radical anion $IV^{\bullet-}$ was also seen in the sequential spectra. Electrochemical reduction of IIa at −0.55 V gave a species with ν(CO) 2055, 2039, 1996 cm^{-1}, whereas the product from cobaltocene reduction had ν(CO) 1992, 1963, 1806 cm^{-1}. This is consistent with the transient electrochemistry, the two species being $IIa^{\bullet-}$ and $IIaZ^{\bullet-}$, respectively.

Discussion

Homonuclear organometallic clusters of the type discussed in this paper have provided an ideal series in which to evaluate the extent to which intracluster electronic interactions can be "turned off" or "turned on" by an appropriate choice of linkage between the metal units. It is clear that there are significant differences in the redox chemistry of those molecules that have *two* Co_3C units and those which have only one. Linkage of $CCo_3(CO)_9$ clusters by unsaturated C–C bonds causes a perturbation of the electronic properties to the extent that new cluster species are derived from EC reactions. This is in contrast to the behavior of those linked via other nonmetal groups such as PR_2[43] and SiR_2,[5,44] which display charge-transfer responses for *individual* cluster redox centers.

In the first group of molecules I the single cluster redox center $CCo_3(CO)_9$ displays a one-electron-reduction process similar to those for other tricobalt carbon clusters which is independent of any other redox process in the molecule. The primary electrode process is a reversible one-electron transfer to form a radical anion. Potentials for this step are comparable with values for other CCo_3 derivatives,[3,11,12] the potentials varying in a predictable way with the electron-donating or -withdrawing character of the apical group.[11,27] A further irreversible reduction to cluster dianions and subsequent fragmentation to $Co(CO)_4^-$ completes the electron transfer sequence. Phosphine or phosphite derivatives $Me_3SiC_2CCo_3(CO)_8L$ and $FcC_2CCo_3(CO)_8L$ also show electrochemical behavior identical with that of other Lewis-base derivatives of the tricobalt carbon cluster.[12]

(43) Alexander, N. C.; Cocks, P. A. Unpublished work, University of Otago.

(44) Borgdorff, J.; Duffy, N. W.; Robinson, B. H.; Simpson, J. *J. Organomet. Chem.*, in press.

Scheme I

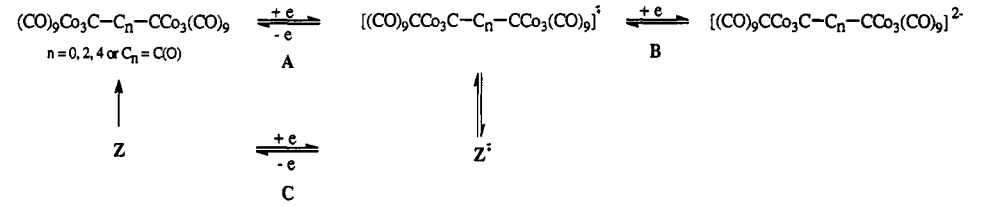

The electron transfer and reactions for *all* molecules containing two $CCo_3(CO)_9$ clusters linked by direct C—C, C—C—C, or –C≡C– bonds II–IV are summarized in Scheme I. A sequence of two one-electron transfers (A and B) at low temperatures for these molecules with identical redox centers is indicative of two interacting cluster entities Clearly the carbyne bridge in II–IV provides a pathway for electronic interaction between clusters. Overlap of the a_1 orbitals from the CCo_3 units and appropriate p_π orbitals on the carbyne chain could perturb the normal orbital topology of a $CCo_3(CO)_9$ cluster, giving a filled molecular orbital encompassing the $Co_3C–C_n–CCo_3$ entity. This would account for the shortened bonds in the carbyne chain, the electron-transfer pathway, and the observation that the potential for the first transfer is similar to that of other CCo_3 derivatives with electron-withdrawing carbyne substituents. This could be an oversimplification, however. The potential for couple A is significantly more positive for IV; this could be attributed to the electronegative group CO in the carbyne chain, but it may be a reflection of subtle, intramolecular, steric interactions involving the equatorial carbonyl groups in the neutral molecule and radical anion, compared to the "linear" species II and III. Once the initial radical anion is produced, the question of whether the valencies are trapped or delocalized arises. Using III as an example, the vibrational trapping energy corresponds to the thermal activation barrier to electron transfer between the parent cluster III and radical anion $III^{\bullet-}$. Mixing of the orbitals of III and $III^{\bullet-}$ would give a delocalized ground state and possibly a magnetically isotropic $III^{\bullet-}$, and the energy required to make the cluster redox sites equivalent is essentially the activation energy for electron transfer between the localized sites. Small changes in geometry or coordination sphere may be sufficient to cause a transition from trapped to delocalized ground states. The electrochemical responses in themselves do not confirm a delocalized ground state in the absence of supporting spectroscopic or magnetic evidence; certainly there is no evidence for mixed-valence behavior. There is a good analogy between the comparative electrochemical behavior of ferrocene/polyferrocenes and $Co_3C/Co_3C_nCCo_3$ species. Ferrocenes bridged by saturated groups normally display a simple oxidation wave with a current proportional to the number of redox centers; this is analogous to the clusters linked by PR_2[43] or SiR′[44] groups. Biferrocene, polyferrocenes, and ferrocenes bridged by unsaturated groups (e.g. –C≡C–) clearly show[6,39,45,46] the transition from discrete to delocalized redox sites occurs in a way similar to that for the linked clusters II–IV. While the separation between the two potentials (A and B) of 0.36 V for III is similar to that for biferrocene (0.33 V),[45] the separation decreased from III to IV to IIa. This variability in the potential could be due to an interaction promulgated by the link, through-space electric field effects, and/or direct electron exchange between redox sites. It is likely that bridge effects dominate in the cluster system, although nonbonded interactions involving the equatorial CO groups cannot be ignored. For example, the distance between redox sites in IIa is considerably shorter than the 7.3 Å in diferrocenylacetylene[6] but the separation between the two redox couples is very similar (0.30 V for IIa and 0.26 V for the ferrocenyl derivative).

In the kinetically controlled regime the formation of the primary radical anion of a linked cluster is followed by an E process giving the dianion, or by a CE process leading to the new species Z which has the associated one-electron reversible couple C. The large shift to negative potentials of couple C when an alkyne group is interpolated between the two cluster centers shows the sensitivity of this couple to the nature of the bridge and/or the distance between the redox sites. Electrochemical data show that the formation of species Z from the radical anion is independent of the second reduction step to the dianion. Chemical or bulk electrochemical reduction of III follow the sequence given in eq 6, and the following points have been established.

(1) There is an overall one-electron transfer from III to $IIIZ^{\bullet-}$.

(2) $IIIZ^{\bullet-}$ undergoes a one-electron-oxidation step to IIIZ.

(3) The redox chemistry is not influenced by intermolecular CO or solvent.

(4) Both Z species have a bridged-carbonyl structure.

(5) The ν(CO) profiles of the two Z species are identical, indicative of closely related cluster geometries, but different from the profiles of the parent cluster III. The difference of approximately 30 cm^{-1} between the spectra of the Z species is consistent with a $Z/Z^{\bullet-}$ relationship.

(6) The $III^{\bullet-} \rightarrow IIIZ^{\bullet-}$ transformation is kinetically preferred over $III^{\bullet-} \rightarrow III^{2-}$ at 293 K.

(7) The metallic skeleton of IIIZ cannot be too different from that of III, as the transformations between the respective neutral molecules or radical anions are reversible both at an electrode surface and in solution.

Unfortunately, the data for IIa and IV were not as comprehensive but, given the similarity in their transient electrochemistry and bulk redox chemistry to those of III, it is reasonable to assume that the structures of the reduced species Z from all linked clusters are related. Nonetheless, the structures must allow for the difference in potential for the couple C between III and IV on the one hand and IIa.

Previous work on derivatives of the tricobalt carbon cluster have shown that a bridged-carbonyl structure is adopted if CO groups are replaced by good electron donors or to relieve steric congestion. Structural isomers involving a terminal ↔ bridged transformation, $MeCCo_3(CO)_8PCy_3$, have been characterized and others identified spectroscopically in tricobalt carbon chemistry.[47] If the $Co_3C–C_n–CCo_3$ entity is stabilized by electron delocalization

(45) Morrison, W. H.; Krogsrud, S.; Hendrickson, D. N. *Inorg. Chem.* **1973**, *12*, 1998.

(46) Morrison, W. H.; Hendrickson, D. N. *Inorg. Chem.* **1975**, *14*, 2331. Brown, G. M.; Meyer, T. J.; Cowan, D. O.; Le Vanda, C.; Kaufman, F.; Roling, P. V.; Rausch, M. D. *Inorg. Chem.* **1975**, *14*, 506.

(47) Matheson, T. W.; Robinson, B. H. *J. Organomet. Chem.* **1975**, *88*, 367.

along the chain, the addition of an electron to the cluster could create a situation where the clusters revert to a bridged-carbonyl configuration to relieve the excess charge and, in the case of III and IV, the nonbonded repulsions between the equatorial carbonyl groups. The IR data are consistent with this suggestion, especially as the energy of the bridging ν(CO) bands is indicative of strong cluster–carbonyl bonding and accounts for the absence of any equilibria involving intermolecular CO and the relatively fast charge transfer. IIIZ$^{\bullet-}$ will be thermodynamically easier to reduce than III$^{\bullet-}$ because of reduced steric congestion in the carbonyl-bridged structure. When the two clusters are separated by –C≡C–, as in IIa, there is no steric congestion, and with the decreased delocalization the result is a more negative reduction potential for species IIZ than for II$^{\bullet-}$ (i.e. $E°$[IIaZ/IIaZ$^{\bullet-}$] < $E°$[IIa^{2-}/IIa$^{\bullet-}$]. Thus, III$^{\bullet-}$ and IIIZ$^{\bullet-}$ are *radical anion isomers* and a representation of their transformation is shown in eq 7.

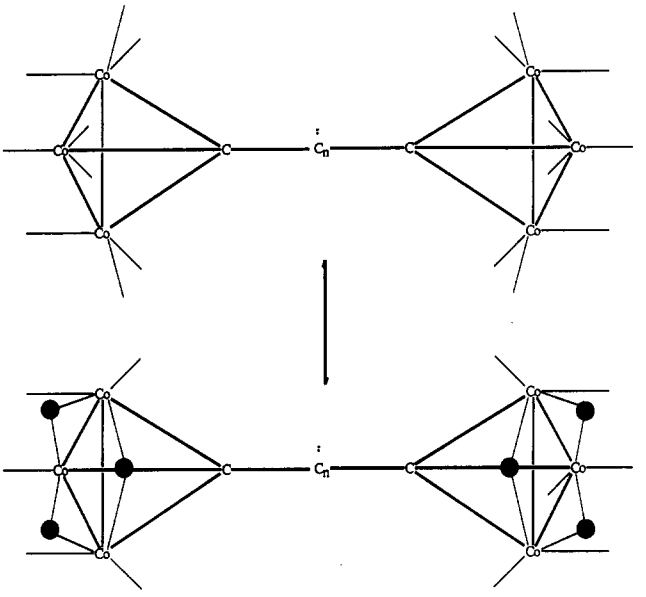

(7)

Many other examples of structural isomerism occurring when organometallic and cluster molecules are reduced or oxidized are known,[39,48] and a related fast interconversion of isomers was found[49] with radical anions of [$(CF_3)_6C_6$-$Co_2(CO)_2L_2$]. Structural relationships between redox-related capped trimetallic systems, especially those studied by Dahl's group, often incorporate the effect of changing occupancy of the LUMO, the addition of an electron distorting the metallic core rather than rearranging the ligand shell.[1,39,50,51] With higher geometries gross changes in the skeletal geometry can occur at rates which may be faster than charge transfer.[1,51] Finally, theoretical and NMR studies[52] suggest that an apical carbonium ion substituent would tilt via direct interaction between the carbonium p_z orbital (not available in the linked clusters if the carbyne chain is unsaturated) and an e-type frontier orbital of the metal framework. These alternatives were considered for the linked cluster investigated in this paper, but the spectroscopic and electrochemical evidence supported a rearrangement of the ligand shell. Preliminary SNIFTIRS data also reinforce this conclusion.[53]

Apart from the electronic and electrochemical consequences of interaction between two clusters described above, recent work has indicated that the thermal stability of the CCo_3 unit is also affected. Thermal degradation of linked clusters such as III produced conducting aggregates, whereas nonconducting powders were obtained from compounds with only one cluster entity (e.g. I).[7] The implications of this observation in the design of precursors for conducting materials are obvious, and further studies on carbyne-linked clusters are planned.

Acknowledgment. We thank Dr. Ward T. Robinson, University of Canterbury, for the X-ray data collection and the University of Otago for the award of a postgraduate scholarship (to G.H.W.).

Registry No. Ia, 138180-57-1; Ib, 131956-31-5; Ic, 138207-62-2; Ie, 129080-65-5; IIa, 29259-33-4; IIb, 138180-56-0; III, 18433-89-1; IV, 19738-50-2; VIb, 143591-05-3; $PhCCo_3(CO)_9$, 13682-03-6; $BrCCo_3(CO)_9$, 19439-14-6.

Supplementary Material Available: Full tables of bond distances and angles, thermal parameters, H atom positional parameters, and weighted least-squares planes and lines for VIb (10 pages). Ordering information is given on any current masthead page.

OM920221G

(48) Connelly, N. G.; Geiger, W. E. *Adv. Organomet. Chem.* **1984**, *23*, 1.

(49) Arewgoda, C. M.; Robinson, B. H.; Simpson, J. *J. Chem. Soc., Chem. Commun.* **1982**, 284.

(50) Simon, G. L.; Dahl, L. F. *J. Am. Chem. Soc.* **1973**, *95*, 2164.

(51) Shriver, D. F., Kaesz, H. D., Adams, R. D., Eds *The Chemistry of Metal Cluster Complexes*; VCH: New York, 1990. Johnston, B. F. G., Ed. *Transition Metal Clusters*; Wiley: New York, 1980.

(52) Schilling, B. E. R.; Hoffmann, R. J. *J. Am. Chem. Soc.* **1982**, *100*, 6274. Edidin, L. T.; Norton, J. R.; Mislow, K. *Organometallics* **1982**, *1*, 561.

(53) Brooksby, P. Unpublished work. Prof. D. Osella (Turin, Italy) has also observed similar room-temperature electrochemistry for III (Osella, D. Personal communication).